

INTRODUCTION

INTRODUCTION

Cellular Organization of the Retina

The major cellular components of the retina are the retinal pigment epithelium cell, the photoreceptor cells, the interneurons, the ganglion cells, and the glial cells.⁽¹⁾

1. Retinal Pigment Epithelium (RPE)

Each adult human retina contains about 3.5 million RPE cells⁽¹⁾ whose diameters vary fourfold between 14 μm in the central retina and 60 μm in the peripheral retina.⁽²⁾ The density of RPE cells is greater in the fovea (5,000 cells/ mm^2) than in the periphery (2,000 cells/ mm^2).⁽³⁾ In the central retina, where RPE cells are most tightly packed, they take the shape of regular hexagonal tiles that form a single layer of cuboidal epithelium. Tight junctions between adjacent RPE cells form the outer blood-retina barrier, an important physiologic barrier to the free flow of molecules between the leaky choriocapillaris and the photoreceptors of the neuroretina.⁽⁴⁻¹⁰⁾

Melanin renders the RPE dark brown to black. Pigmentation of the RPE is a rapid process that begins at about 35 days of gestation and is complete within approximately 1 week.⁽¹¹⁾

2. Photoreceptors

The photoreceptors are the sensors of the visual system that convert the capture of photons into a nerve signal in a process called phototransduction.⁽¹²⁾ The human retina contains approximately four to five million cones and 77–107 million rods.⁽¹²⁻¹⁵⁾ Only cones are found in the foveola, whereas rods predominate outside the foveola in the remaining fovea and all of the peripheral retina. Among the three cone photoreceptors, red cones (63% or 2.9 million) are more common than green (32% or 1.4 million) and blue cones (5% or 0.2 million).⁽¹⁶⁾

3. Interneuron Cells

Interneurons in the inner nuclear retinal layer connect the photoreceptor layer with the ganglion cell layer. These interneurons consist of the bipolar, horizontal, amacrine, and interplexiform cells, which form complex neuroretinal circuitries in the outer and inner plexiform layers (IPLs) that process the photoreceptor signal and transmit this information to the ganglion cell layer.^(17,18)

4. Ganglion Cells(GC)

Finally, the ganglion cells are responsible for transmitting visual information from the retina to the brain. The ganglion perikarya are located in the ganglion cell layer, while their dendrites make contact with bipolar and amacrine cells in the IPL. Up to 20 different ganglion cell types have been described in the human retina – the two best known types are the midget and the parasol cells, which make up about 80% of ganglion cell population.⁽¹⁴⁾

5. Glial Cells

Four glial cell types are found in the retina: Müller cells, astrocytes, microglia, and occasionally, oligodendrocytes. *Müller cells* are the main glial cells of the retina.⁽¹⁹⁻²²⁾ Their perikarya are located in the inner nuclear layer with cell processes that span the entire neuroretina.⁽¹⁹⁾ The proximal extensions of Müller cells expand and flatten to form

so-called *endfeet* whose basal lamina forms the *inner limiting membrane*. Distally, Muller's extensions give rise to the outer limiting membrane by forming a series of junctional complexes. Lateral extensions of Muller cells surround the retinal neurons.⁽²³⁾

General Histological Organization of the Retina

The retina is the neurosensory component of the eye. Its outer part is supplied by a vascular layer, the choroid, and protected by a tough outer layer, the sclera. The cellular elements of the retina are arranged and adapted to meet the functional requirements of the different regions of the retina. The regional differentiation of the retina is a process of slow maturation that takes several years to be completed.⁽¹⁾

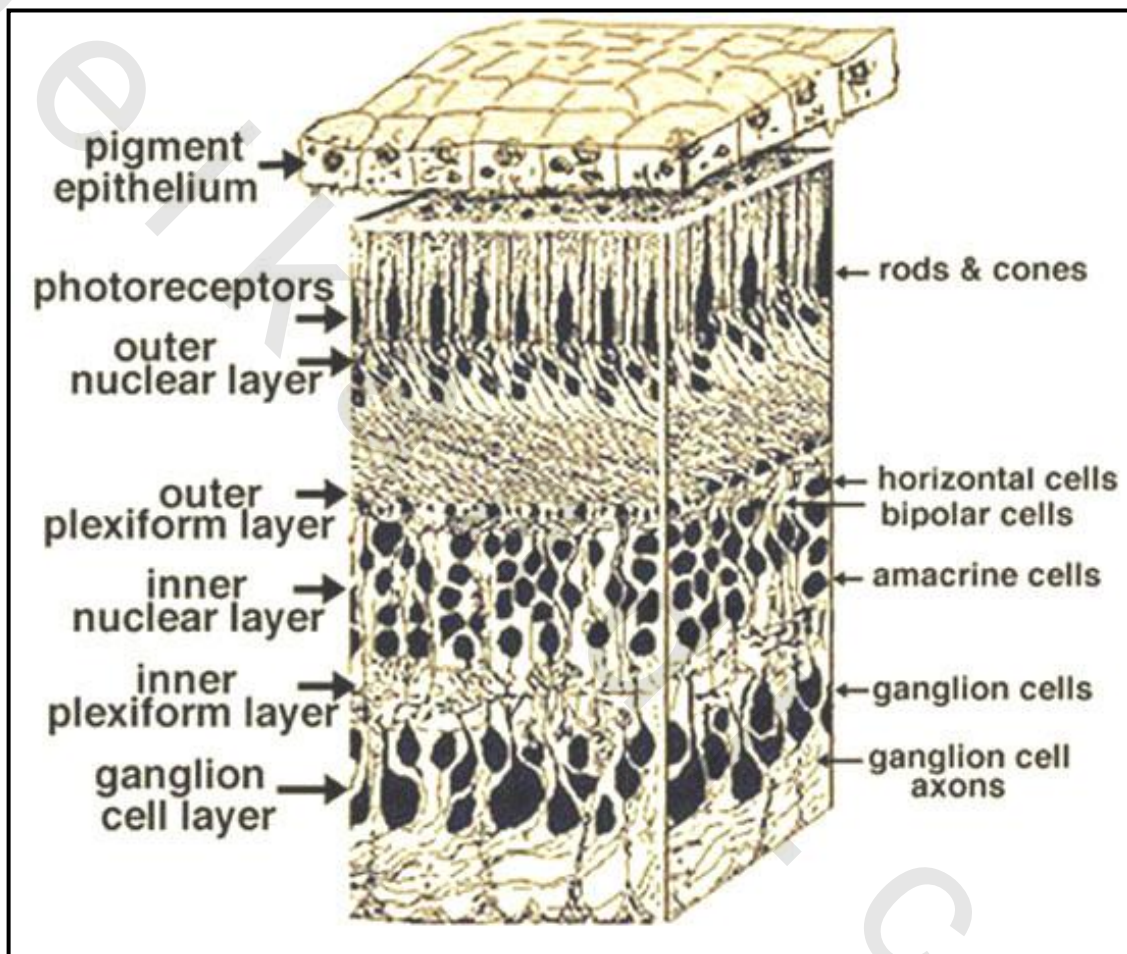


Fig. (1): Three dimensional 3-D block of a portion of human retina.⁽²⁴⁾

The retina has ten distinct layers. From farthest to closest from the vitreous body. That is:

1. Retinal Pigment Epithelium (RPE)

This layer consists of a single layer of cuboidal epithelium.⁽⁴⁻¹⁰⁾

2. Photoreceptor Layer

Rods and cones are tightly stacked together into a single palisading layer of photoreceptors.^(12,13,15,25-27)

3. External Limiting Membrane (ELM)

It is created by junctional complexes between adjacent Müller cells as well as between Müller and photoreceptor cells.^(28,29)

4. Outer Nuclear Layer (ONL)

The outer nuclear layer contains the nuclei of the photoreceptor cells.⁽³⁰⁾

5. Outer Plexiform Layer (OPL)

The OPL has two components: the axons of the photoreceptor, bipolar and horizontal cells and their synaptic connections. The axons of the photoreceptor cells form a specialized structure, Henle's fiber layer, in the central retina.⁽³¹⁾

6. Inner Nuclear Layer (INL)

This layer harbors the nuclei of: the horizontal, the bipolar, the amacrine, the interplexiform, and the Müller cells.^(14,19,32)

7. Inner Plexiform Layer (IPL)

The IPL Contains the synapses between bipolar, amacrine, and ganglion cells.⁽³³⁾

8. Ganglion Cell Layer (GCL)

This layer contains the nuclei of ganglion cells and other cell types, including “displaced” amacrine cells, astrocytes, endothelial cells, and pericytes.^(12,34-36)

9. Nerve Fiber Layer (NFL)

Ganglionic axons travel towards the optic nerve head within the nerve fiber layer.^(17,37)

10. Inner Limiting Membrane (ILM)

The innermost processes of the Müller cell enlarge and flatten on the vitreal side to form the inner limiting membrane.⁽²³⁾

Anatomy of the retina

The adult *posterior pole* (anatomic macula or area centralis) is about 4.5–6 mm in diameter, centered on the fovea, and located between the superior and inferior temporal arcades. The *macula* (anatomic fovea centralis) is located approximately 3 mm temporal to the optic disc and is about 1.5 mm, or one disc size, in diameter.⁽³⁶⁾ The presence of xanthophyll, a yellow carotenoid pigment, gives the region its name – the macula lutea.⁽¹⁶⁾

The most central part of the macula, the *fovea* (anatomic foveola), is formed by a central, circle 0.35 mm wide depression and represents the retinal region of greatest visual acuity.⁽¹⁶⁾ (fig. 2) Clinically, it is recognized by the foveal reflex, blunting or loss of which may indicate early macular disease. The foveola is demarcated by a sloping wall, the clivus, which contributes to the annular light reflex that is seen in children and young adults. The foveola has the highest density of cone photoreceptors (199,000/mm²), which are narrowed and elongated in this location to maximize light detection further.⁽³⁸⁾ The long axons of the foveal cones form Henle's layer as they radiate out of the central depression. The fovea develops by an opposing process of outward displacement of the cells of the inner nuclear and ganglion cell layers, while the cone photoreceptors migrate toward the center.⁽³⁹⁻⁴¹⁾ Rod photoreceptors are excluded from the foveal outer retina (“rod-free zone”). As a result, the foveola contains only

cone photoreceptors and some Müller cells. The central 500 μm of the fovea contains no retinal capillaries (the *foveal avascular zone [FAZ]*), making the fovea dependent on blood supply from the choriocapillaris. The exact extent of the FAZ can be delineated with accuracy only by fluorescein angiography. Retinal blood vessels from the temporal retina do not cross the central fovea but arc around it.⁽³⁶⁾

The *peripheral retina* comprises the remaining retina outside the temporal retinal arteries. Anatomically, the peripheral retina possesses only one layer of ganglion cells. The *ora serrata* delineates the anterior termination of the sensory retina and the beginning of the pars plana of the ciliary body. At this junction, the sensory retina is reduced to a single cell layer which, anteriorly, becomes the nonpigmented ciliary epithelium whereas the retinal pigment epithelium (RPE) is replaced by pigmented ciliary epithelium.⁽³⁶⁾

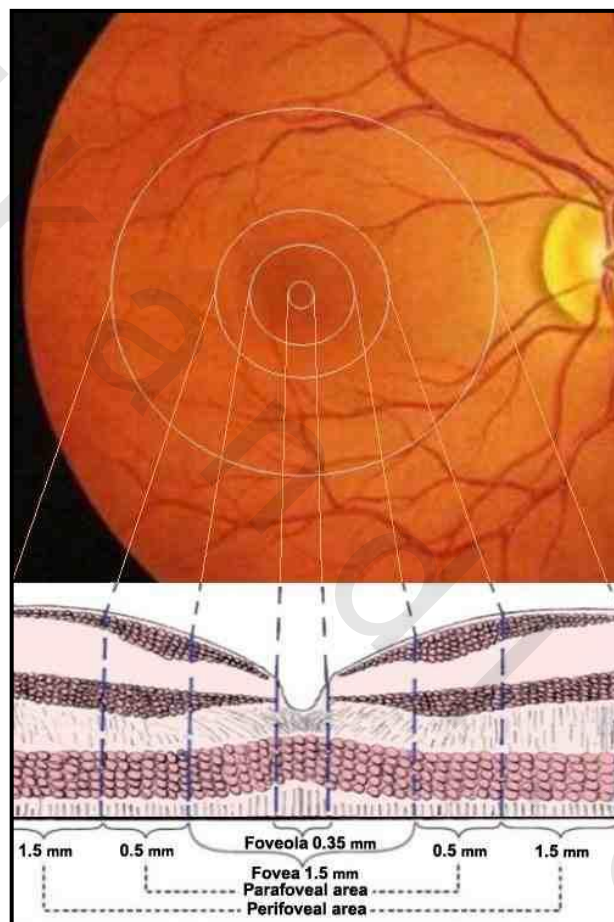


Fig. (2): Anatomy of the retina.⁽⁴²⁾

Central retina compared to peripheral retina

Central retina close to the fovea is considerably thicker than peripheral retina (compare Figs. 3 and 4). This is due to the increased packing density of photoreceptors, particularly the cones, and their associated bipolar and ganglion cells in central retina compared with peripheral retina.⁽²⁴⁾

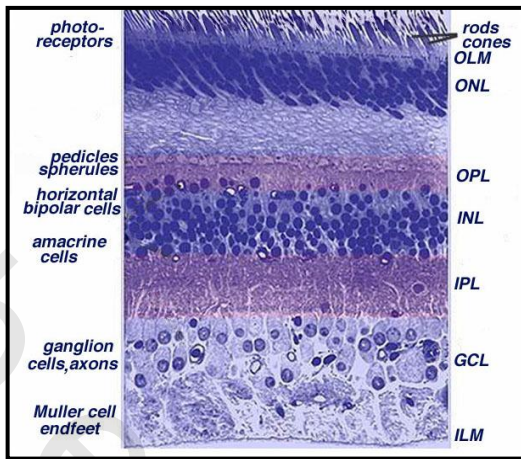


Fig. (3): Light micrograph of a vertical section through human central retina.⁽²⁴⁾

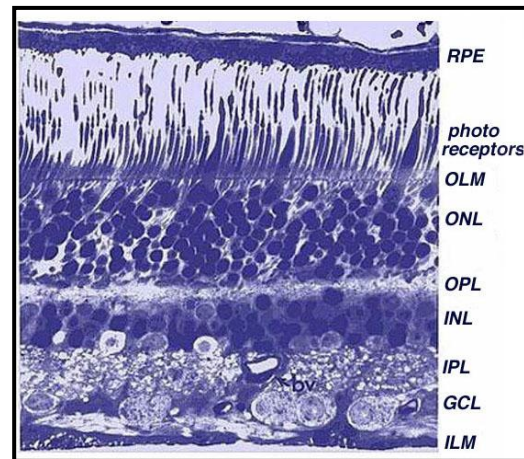


Fig. (4): Light micrograph of a vertical section through human peripheral retina.
(24)

- The outer layer (ONL), composed of the cell bodies of the rods and cones is about the nuclear same thickness in central and peripheral retina. However in the peripheral the rod cell bodies outnumber the cone cell bodies while the reverse is true for central retina. In central retina, the cones have oblique axons displacing their cell bodies from their synaptic pedicles in the outer plexiform layer (OPL). These oblique axons with accompanying Muller cell processes form a pale-staining fibrous-looking area known as the Henle fibre layer. The latter layer is absent in peripheral retina.⁽²⁴⁾
- The inner nuclear layer (INL) is thicker in the central area of the retina compared with peripheral retina, due to a greater density of cone-connecting second-order neurons (cone bipolar cells) and smaller-field and more closely-spaced horizontal cells and amacrine cells concerned with the cone pathways. Cone-connected circuits of neurons are less convergent in that fewer cones impinge on second order neurons, than rods do in rod-connected pathways. **(Fig.3)**⁽²⁴⁾
- A remarkable difference between central and peripheral retina can be seen in the relative thicknesses of the inner plexiform layers (IPL), ganglion cell layers (GCL) and nerve fibre layer (NFL) (Figs. 3 and 4). This is again due to the greater numbers and increased packing-density of ganglion cells needed for the cone pathways in the cone-dominant foveal retina as compared the rod-dominant peripheral retina. The greater number of ganglion cells means more synaptic interaction in a thicker IPL and greater numbers of ganglion cell axons coursing to the optic nerve in the nerve fibre layer (Fig. 3).⁽²⁴⁾

Special histological organization of the fovea

Though the posterior pole (the anatomic macula) makes up less than 4% of the entire retina, it accounts for all central and most photopic vision.⁽⁴³⁾ Because of its special histological organization, the posterior pole is subdivided into four concentric regions: the perifovea, the parafovea, the foveal slope, and the foveola.⁽⁴³⁾ The *perifovea* is the outermost region of the anatomic macula that borders the peripheral retina. It is rich in retinal blood vessels and has a high rod–cone ratio of 33–130:1, an increased cone density compared with the peripheral retina, and a ganglion cell layer that is greater than a single cell layer in thickness. The *parafovea* is located between the fovea and the perifovea. It contains less retinal vessels, has a reduced rod: cone ratio of 4:1, and has the highest

density of ganglion cells. The fovea contains the *foveola*, a flat central depression in the fovea and the site of maximum visual acuity. The foveola is surrounded by the *foveal slope* or clivus. Importantly, the clivus marks the switch from vascular to avascular retina (the FAZ) and from rod-dominated to cone-dominated retina⁽⁴³⁾ (Fig. 5).

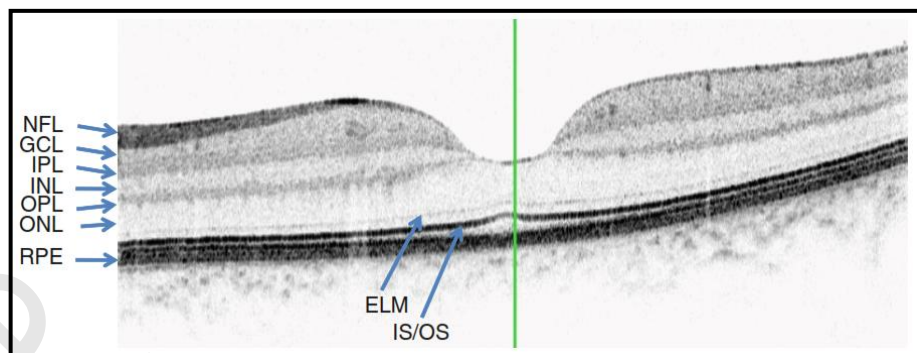


Fig. (5): Spectralis™, Heidelberg Engineering, Germany). *NFL* nerve fiber layer (left papillomacular bundle); *GCL* ganglion cell layer; *IPL* inner plexiform layer; *INL* inner nuclear layer; *OPL* outer plexiform layer; *ONL* outer nuclear layer; *ELM* external limiting membrane; *IS/OS* inner/ outer segment junction; *RPE* retinal pigment epithelium.⁽⁴³⁾

There is a progressive increase in the neurosensory retinal thickness from 30 weeks postmenstrual age (PMA) to 16 years of age. Pre-term infants demonstrate a shallow foveal pit indenting inner retinal layers (IRL) and short undeveloped foveal photoreceptors. At term, further IRL displacement from the pit and peripheral photoreceptor lengthen; the elongation of inner and outer segment (IS and OS) separates the IS band from retinal pigment epithelium. Foveal IS and OS are shorter than peripheral for weeks after birth. By 13 months of age, foveal cone cell bodies deepened, Henel's fiber layer (HEL) thickens, and IS/ OS length equal peripheral. At 13 to 16 years, the fovea is fully developed with a full complement of Spectral domain optical coherence tomography SD-OCT bands; cone cell bodies become more deep and have thin, elongated and tightly packed IS/OS.⁽⁴⁴⁾

Optical coherence tomography (OCT)

OCT is a diagnostic imaging technology that provides cross-sectional images of biological tissues. In ophthalmology, OCT can perform "optical biopsy" noninvasively, imaging the retina with a resolution higher than any other imaging modality other than histology. Now, nearly two decades since its introduction, OCT has become indispensable for research, screening, diagnosing, and monitoring diseases of the macula and optic nerve head. OCT was developed by researchers at the Massachusetts Institute of Technology and collaborators and was first reported in Science in 1991.⁽⁴⁵⁾

Principles of OCT

OCT imaging is analogous to B-scan ultrasonography, except that OCT measures light rather than acoustic waves.

Time domain OCT

OCT is performed by measuring the echo delay and intensity of backscattered light from the internal tissue microstructure. Because the echo time delays of light are too fast to measure directly, an optical correlation technique, known as Michelson low coherence interferometry,

is used. Low-coherence light from a superluminescent diode (SLD) is directed through a beam splitter and divided into a sample beam that is focused onto the patient's retina and a reference beam that travels a calibrated delay path (Fig. 6). Light backscattered by retinal structures interferes with light from the reference beam, and the interference of the echoes is detected to measure the backscattering signal versus delay or depth.⁽⁴⁵⁾

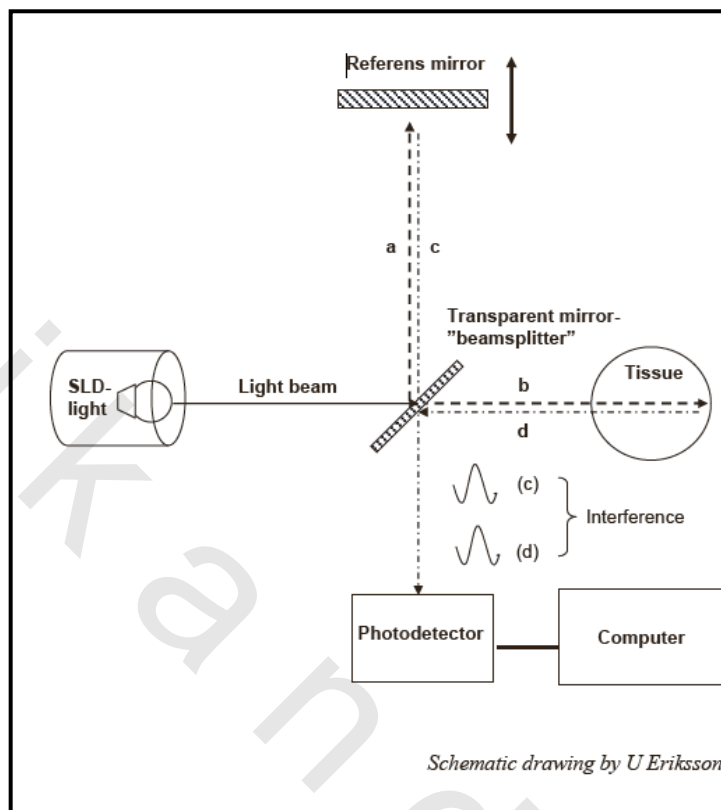


Fig. (6): Schematic presentation of an Optic interferometer (Michelsons interferometer). SLD= Super luminescent diode source. a=beam reflected towards the reference mirror. b= beam passing through the beam splitter to the tissue sample. c=beam reflected back from the reference mirror. d=beam reflected back from the sample. Signal is recorded in the photodetector, and transferred to a computer for signal analysis.⁽⁴⁶⁾

Conventional OCT systems use time-domain (TD) detection, in which the reference mirror is mechanically scanned to produce axial scans (A-scans) of the light echoes vs depth. The optical beam is scanned in the transverse direction to obtain 2-D cross-sectional images (B-scans) of microstructure. Stratus OCT (Carl Zeiss Meditec, Dublin, Calif), the third-generation instrument, uses TD detection and acquires 400 A-scans per second.⁽⁴⁵⁾

The axial image resolution depends on the bandwidth of the light source. Stratus OCT utilizes a near-infrared superluminescent diode light source centered at ~820 nm with a ~25 nm bandwidth to attain an axial resolution of ~8 to 10 μm in the eye. Conversely, transverse resolution is determined by size of the focused optical beam.⁽⁴⁵⁾

The restricted speed of OCT with TD detection, however, limits image quality and retinal coverage. Eye movements introduce motion artifacts that require digital processing, which may obscure important pathologic features. The number of A-scans that can be acquired is limited, restricting retinal coverage and increasing sampling errors for detecting focal pathologies.⁽⁴⁶⁾

Spectral domain OCT (SD- OCT)

Advances in detection techniques, known as Fourier-domain (FD) or spectral-domain (SD) detection, helped overcome many of the speed limitations of TD detection. SD/FD detection uses an interferometer with a high-speed spectrometer (Figure 7) and measures light echoes from all time delays simultaneously, rather than sequentially as in TD detection. This enables increases of more than 50 times in axial scanning speeds. A similar technique, swept source/FD detection, also known as optical frequency-domain imaging, uses a frequency-swept light source and a photodetector instead of spectrometer.⁽⁴⁷⁻⁴⁹⁾

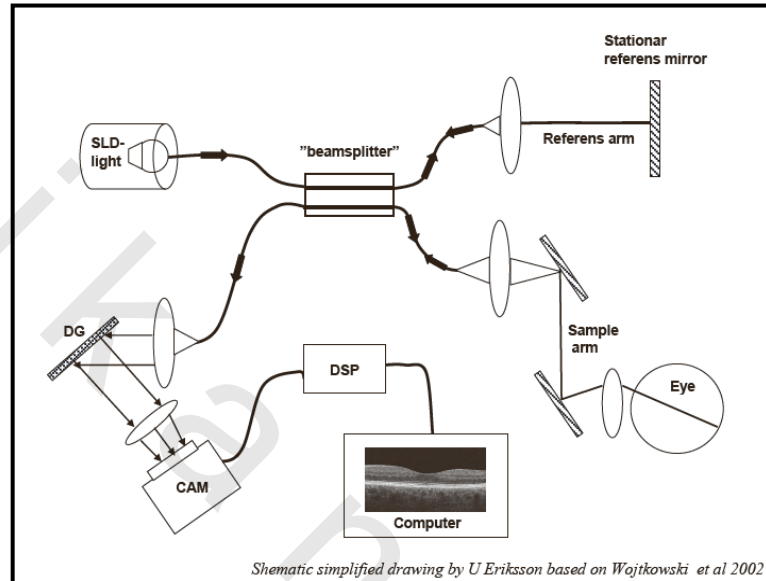


Fig. (7): Simplification of a spectral domain OCT setting. SLD=Super luminescent light source. The reference mirror is fixed. DG=diffraction grating. A full field detector (CAM) act as spectrometer. DSP= digital signal processing.⁽⁵⁰⁾

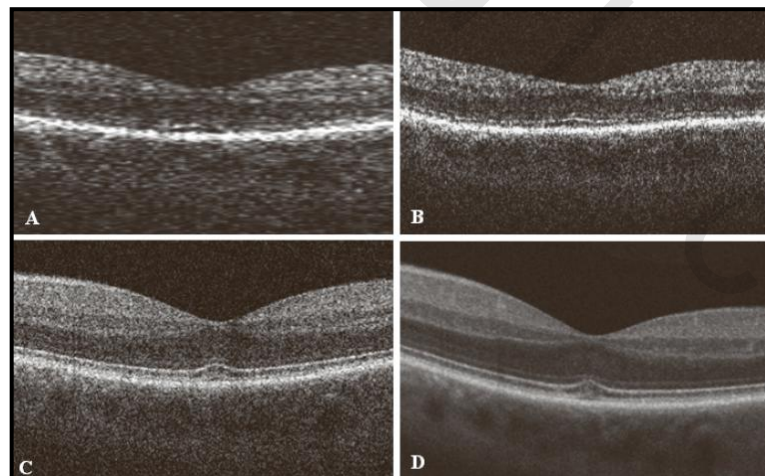


Fig. (8): Image A is a single B-scan from the Stratus fast program (128 A-scans) and B from the standard (512 A-scans) of a normal macula. Image C is a B-scan from Cirrus, (512 A-scans), of the same macula. Note the better quality compared to Stratus standard (B) composed from equal number of A-scans. This improvement is primarily due to the faster acquisition speed in Cirrus. Image D is a Cirrus image further improved by “averaging” of multiple scans.⁽⁵⁰⁾

The faster acquisition speeds of OCT with SD/FD detection improve image quality by reducing eye motion artifacts, resulting in a more accurate portrayal of the true retinal contour. Furthermore, the improved transverse sampling and increased axial resolution enable more detailed images to be produced without having to increase power-exposure levels. Faster acquisition speeds also enable greater retinal coverage and more precise registration of OCT images with fundus features. While Stratus OCT mapped the macula based on interpolated data from six radial line scans, SD/FD OCT enables dense raster scans composed of closely spaced B-scans acquired as 3D-OCT data sets. Clinically, this enables physicians to identify focal lesions near the fovea in poorly fixating patients.⁽⁵¹⁾

Three-dimensional OCT also improves the quantification of thickness and volume. By interpolating less than TD OCT, greater accuracy in thickness measurements may be attained with SD/FD OCT.⁽⁵¹⁾ (Fig. 8) is an example of different image qualities that can be obtained with the stratus and cirrus OCT.⁽⁵⁰⁾

Ultrahigh-Resolution OCT (UHR-OCT)

In 1999, ultrahigh-resolution OCT, with an axial resolution of 2 to 3 μm was first demonstrated. This resulted from improvements in light-source technology, replacing the SLD with a broad-bandwidth femtosecond titanium: sapphire laser and later with multiplexed SLDs. This advance enabled improved delineation of intraretinal layers, enabling "optical biopsy" of the retina.^(52,53)

These technical difficulties and the costly laser, have been the major drawbacks in the commercialization of UHR-OCT.⁽⁵³⁾

Spectral domain /fourier domain OCT (SD/FD)

With the advent of broad-bandwidth, SLD light sources and recognition of performance gains offered by SD/FD detection, at least seven manufacturers have introduced OCT instruments since 2006. These instruments offer similar specifications, with axial image resolution in the ~ 4 to 7 μm range and acquisition speed in the 20,000 to 40,000 A-scans per second range. All models offer the benefits of improved coverage and precise registration over OCT with TD detection. Some units are designed as standalone OCT (Bioptigen SD OCT [Research Triangle Park, NC], Optopol/ Reichert Copernicus, [Zawierce, Poland], Optovue RTVue-100 [Fremont, CA], Carl Zeiss Meditec Cirrus HD-OCT [Dublin, CA]), while others combine OCT with microperimetry (Opko/OTI Spectral OCT/SLO [Toronto, Canada]), color fundus photography (Topcon 3D OCT-1000 [Paramus, NJ]), Fluorescein Angiography, Indocyanine green angiography, autofluorescence, or red-free imaging (Heidelberg Spectralis HRA+OCT [Heidelberg, Germany]). Most models offer importation of images from other instruments for direct comparison with OCT images.⁽⁵⁴⁾

Different products have different ergonomic features as well as differences in software. Scan protocols can differ in type and density, depending on the clinician's preference for sampling resolution versus the patient's ability to fixate reliably for a long time. Motion artifacts and registration are dealt with through software, although one model (Spectralis HRA+OCT) employs eye tracking.

Segmentation algorithms used to define layer boundaries for macular thickness measurements vary as well. Retinal thickness measurements on the Stratus OCT were previously defined from the internal limiting membrane to the IS/OS junction.⁽⁵⁴⁾ While

circus segmentation algorithm placed the PRE boundary line just below the front edge of the hyper reflective band interpreted as the anatomic RPE. The Spectralis OCT typically segment the back edge of the same hyper reflective band, leading to somewhat thicker retinal thickness measurements.⁽⁵⁵⁾

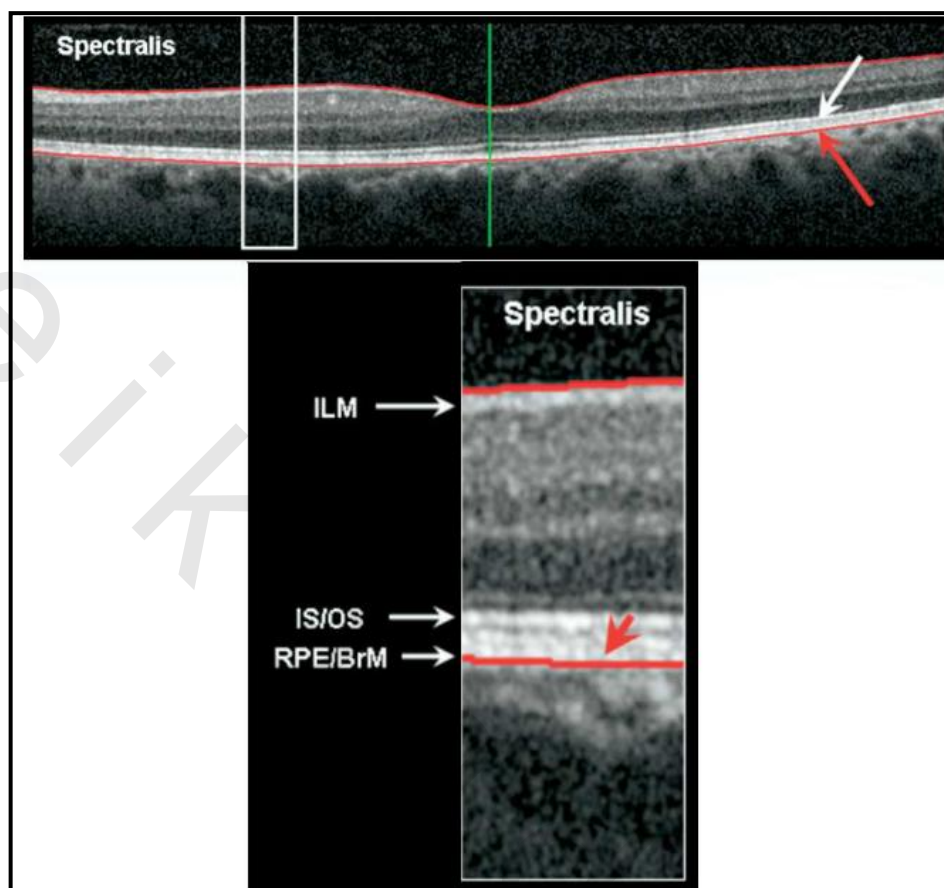


Fig. (9): Demonstration of macular thickness segmentation algorithm by Spectralis. (Top) the white arrow points to the photoreceptor inner/outer segment junction (IS/OS). The red arrow points to the approximate junction of RPE/Bruch membrane BrM . The vertical white rectangle at left shows the area enlarged in the bottom figure. (Bottom) White arrows show approximate level of ILM, IS/OS, and RPE/BrM. Red arrows point to outer retina segmentation line seen to overlie the RPE/BM junction.⁽⁵⁶⁾

SPECTRALIS OCT (Heidelberg Engineering, Heidelberg, Germany)

The Spectralis (Fig. 10) is one of the newest OCTs based on spectral-domain technology. It combines a scanning laser ophthalmoscope (SLO) with OCT to produce tracking laser tomography that scans at 40000 A-scans per second. Its optical depth resolution is 7 μm , the digital depth resolution 3.5 μm , and the transverse resolution is 20 μm .⁽⁵⁷⁾



Fig. (10): The Spectralis OCT. (Image courtesy of Heidelberg Engineering GmbH).⁽⁵⁸⁾

One beam constantly images and tracks the fundus and acts as a reference, guiding the second beam of light precisely to position the cross-sectional OCT scan.⁽⁵⁹⁾ This real time eye tracking enables a highly repeatable alignment of OCT and fundus images that can be displayed either in grayscale or false color and allows acquisition of 1 to 100 B-scans at the same location (Automatic real-time mode or ART), facilitating removal of speckle noise artifact by frame averaging.⁽⁶⁰⁾ This scanning precision results in very high repeatability and reproducibility with a very small measurable change ($1.5 \mu\text{m}$) and coefficient of variation (COV; 0.53%), thereby allowing repeat scans of identical locations at different time points allowing precise follow-up of patients.⁽⁶¹⁾

Regarding macular thickness measurement, the Spectralis OCT offers several volume scan protocols with varying scan density (Fig. 11). Studies showed that Spectralis OCT macular thickness measurements in healthy subjects showed good protocol interchangeability for the different macular volume scan protocols (fast, dense and detail).

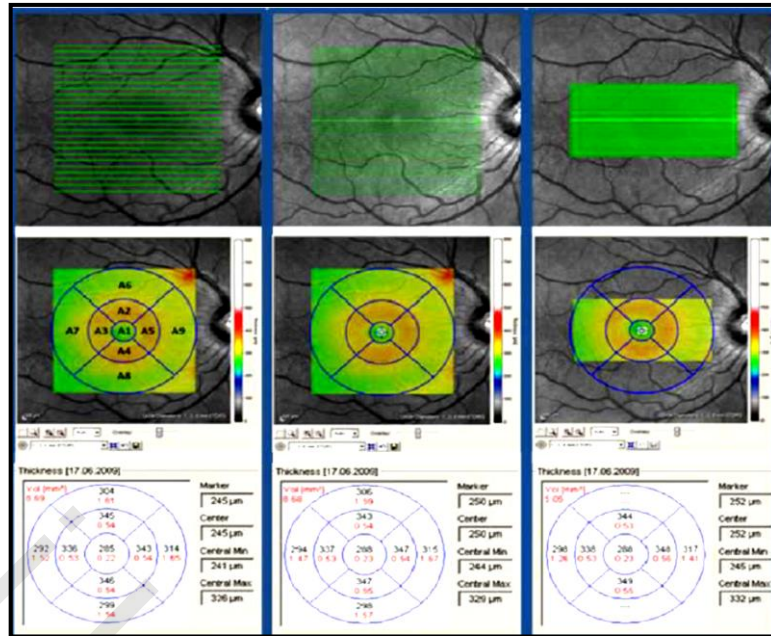


Fig. (11): Different volume scans for macular thickness measurement in the Spectralis OCT. Top row: volumetric scans through the macula. To the left: Fast protocol; scanning area $20^{\circ} \times 20^{\circ}$, 25 B-scan sections spaced 240 μ m apart, 9 Frames OCT ART Mean. In the middle: Dense protocol; scanning area $20^{\circ} \times 20^{\circ}$, 49 B-scan sections spaced 120 μ m apart, 16 Frames OCT ART Mean. To the right: Detail protocol; scanning area $10^{\circ} \times 20^{\circ}$, 97 B-scan sections spaced 30 μ m apart, 16 Frames OCT ART Mean. Bottom row: the corresponding false colour maps with macular areas corresponding to those used in the Early Treatment Diabetic Retinopathy Study (ETDRS) and numeric printouts. The diameters of the three circles are 1, 3, and 6 mm.⁽⁶²⁾

Normal macular OCT scan

The OCT image closely approximates the histological appearance of the macula and, for this reason, it has been referred to as an *in vivo* optical biopsy. With the increase in the axial resolution of the new SD-OCT instruments (5–8 μ m) and the ultrahigh-resolution OCT (2 μ m), it has become possible to correlate OCT images accurately with histological features of the retina.⁽⁶³⁾

The first detected layer in most OCT scans is the ILM that appears as a hyper-reflective layer at the vitreoretinal interface. In some patients, the posterior hyaloid can be seen above the ILM as a hyper-reflective layer. Within the retina, the retinal nerve fiber layer and the plexiform layers (both inner and outer) are seen as hyper-reflective while the ganglion cell layer and the nuclear layers (both inner and outer) are hyporeflective. A recent study demonstrated that the incidence of the light beam could affect the appearance of Henle's fiber layer by OCT, resulting in a thin hyper-reflective layer corresponding to the photoreceptor synapses or a thicker hyper-reflective layer corresponding to photoreceptor axonal extensions enveloped by the outer cytoplasm of Müller cells.⁽⁶²⁾ The retinal vessels may sometimes be seen on OCT images as circular hyper-reflective structures located in the inner retina, with a vertical shadow or reduced reflectivity extending into deeper layers.

Outside the central fovea, commercially available SD-OCT instruments typically resolve four bands in the outer retina. There is discordance between different authors regarding which anatomical structure correlates with each band.^(64,65) The innermost band has been attributed to the ELM. This band is typically thinner and fainter than the others. The nomenclature for the middle two bands has much less supportive evidence. The second of the four bands has been commonly ascribed to the boundary between the IS/OS of the photoreceptors and the third band is referred to as either the OS tips or as Verhoeff's membrane.^(66,67) A recent study suggested that the second band was the ellipsoid section of the photoreceptors (inner segment) instead of the IS/OS junction and that the third band appears to correspond to the contact cylinder between the RPE apical process and the external portion of the cone outer segment. This band typically merges with the fourth band in the central fovea and this is explained by a greater height of the contact cylinder of the cones and RPE outside the fovea.⁽⁶⁵⁾ The fourth hyper-reflective outer retinal band is attributed to the RPE, with potential contribution from Bruch's membrane and choriocapillaris, with abundant experimental and clinical evidence supporting this designation.⁽⁶⁶⁻⁶⁹⁾

The high axial resolution and the different scan patterns offered by SD-OCT provide comprehensive structural information that can be used to map retinal layer thicknesses and perform volumetric analyses.⁽⁷⁰⁾

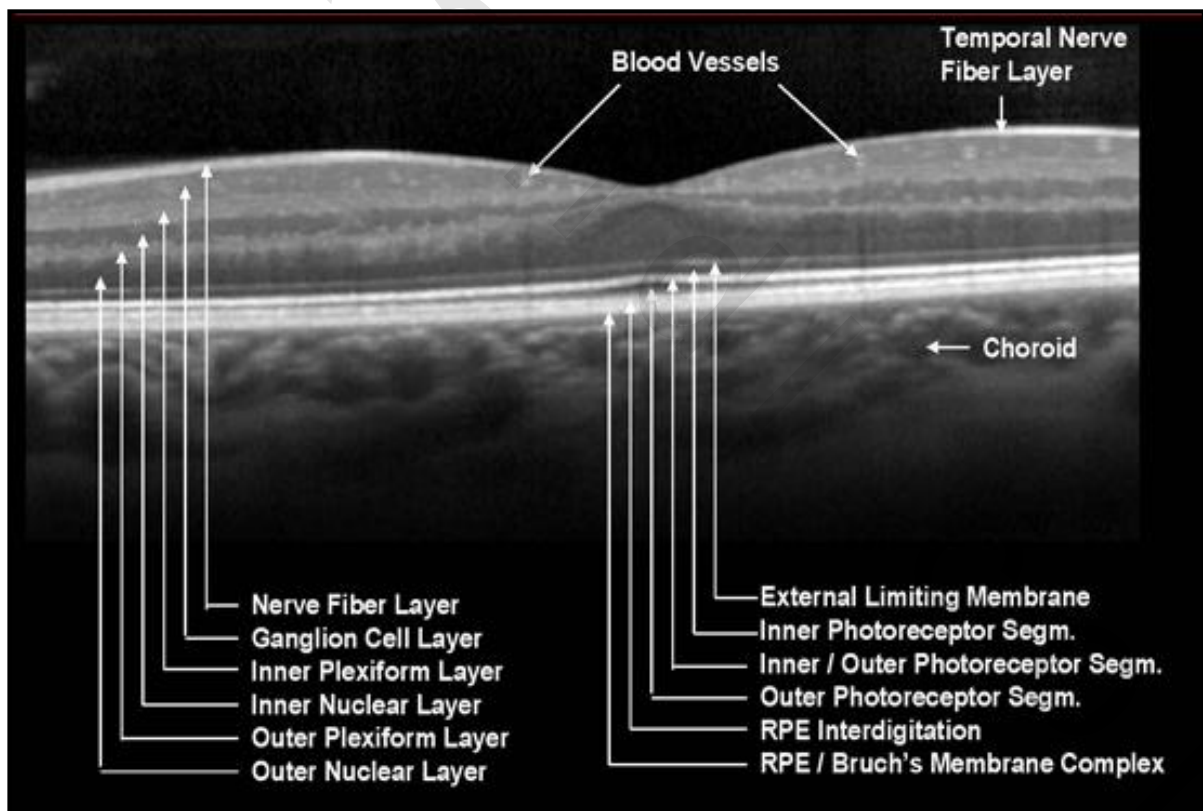


Fig. (12): OCT image of a healthy macula. (Image courtesy of Heidelberg Engineering GmbH).⁽⁵⁸⁾

Importance of macular thickness using OCT in pediatric age group Retinopathy of Prematurity (ROP)

Baker et al used OCT to study eyes with ROP that had no significant macular pathology on ophthalmoscopy and demonstrated subclinical changes in foveal anatomy, including relative loss of foveal depression, increased macular thickness, and preservation of inner retinal layers within the fovea.⁽⁷¹⁾

Coats' disease

Kaul et al used OCT to quantify the resolution of cystoid macular oedema (CME) in a 16 years old boy with Coats' disease after intravitreal injection with anti-vascular endothelial growth factor (VEGF) (pegaptanib sodium).⁽⁷²⁾ Using OCT, the absence of vitreoretinal traction was confirmed in a full thickness macular hole encountered in a 9 years old boy with Coats' disease.⁽⁷³⁾



Fig. (13): Fundus photograph (A) and optical coherence tomography (OCT) image (B) of the right eye of a 4 years old girl with Coats' disease. Fundus picture reveals dilated and telangiectatic blood vessels with exudation and severe lipid deposition in the macula. Longstanding submacular exudates stimulated in-growth of fibrous tissue or blood vessels, which lead to retinal pigment epithelial (RPE) migration and hyperplasia, the formation of RPE detachment seen on OCT. Intraretinal fluid collection is noted as well.⁽⁷⁴⁾

Choroidal neovascularization

By using OCT, they were able to quantitatively prove that anti-VEGF agents were effective in the treatment of pediatric choroidal neovascular membranes in this case series.⁽⁷⁵⁾

Toxoplasmosis

OCT features included retinal thinning, retinal pigment epithelial hyper-reflectivity, excavation, intraretinal cysts, and fibrosis.⁽⁷⁶⁾

Shaken-baby syndrome

The most frequent OCT findings in shaken-baby syndrome were pre-retinal and multilayered retinal hemorrhages, perimacular folds, focal posterior vitreous separation with multilayered hemorrhagic retinoschisis, disruption of the foveal architecture, and foveolar detachment.⁽⁷⁷⁾

Inherited retinal disorders

Albinism

The abnormalities noted on OCT were the persistence of an abnormal highly reflective band across the fovea, multiple inner retinal layers normally absent at the center of the fovea, and loss of the normally thickened photoreceptor nuclear layer usually encountered at the fovea.⁽⁷⁸⁾

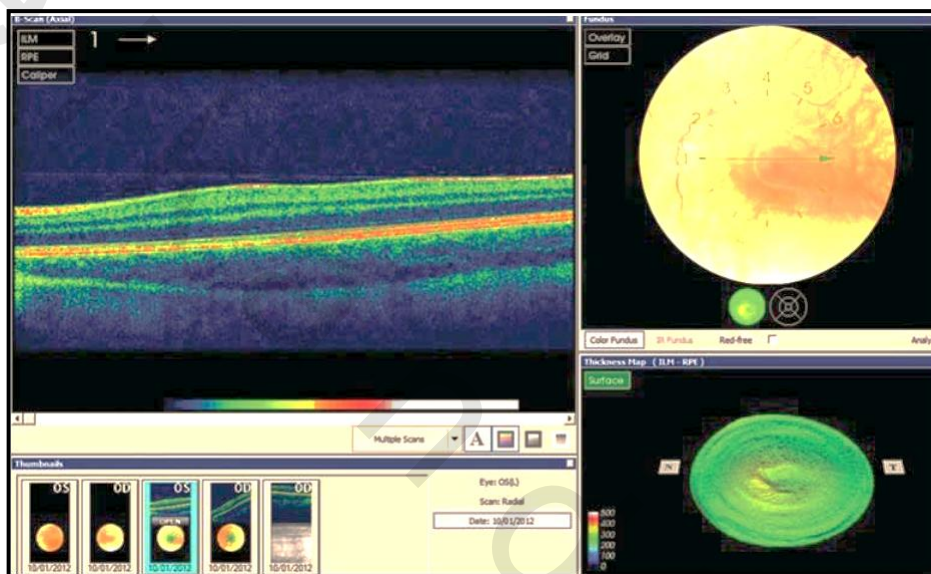


Fig. (14): Fundus photograph and optical coherence tomography (OCT) image of the left eye of an 8 years old boy with oculocutaneous albinism. Note the hypopigmented fundus. OCT demonstrated the persistence of an abnormal highly reflective band across the fovea, multiple inner retinal layers normally absent at the center of the fovea, and loss of the normally thickened photoreceptor nuclear layer usually encountered at the fovea.⁽⁷⁸⁾

Leber congenital amaurosis

OCT may function as an objective diagnostic tool by detecting foveal and extrafoveal photoreceptor loss early in the course of Leber congenital amaurosis.⁽⁷⁹⁾

Best's disease

OCT can help define the characteristics of this “egg yolk” appearance. Furthermore, OCT has the ability to visualize CME that is associated with inherited retinal dystrophies (Figure 16).^(80,81)

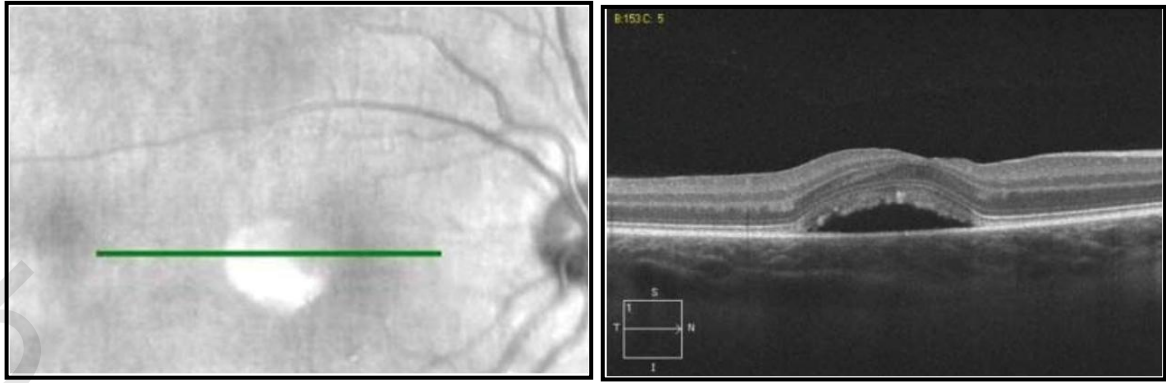


Fig. (15): Cirrus high-definition optical coherence tomography (OCT) generated fundus image (A), and OCT image (B) of the right eye of a 9 years old boy with Best's disease: Yolk-like (vitelliform) lesion is noted in the central macula.^(80,81)

Uveitis

Stratus OCT was able to detect macular edema in 25% of the eyes, most of which was mild and not clinically evident.⁽⁸²⁾

Tumors

Shields et al used OCT in the evaluation of pediatric fundus lesions in retinal capillary hemangioma, astrocytic hamartoma, and retinoblastoma.⁽⁸³⁾

Critical OCT changes in retinal nerve fiber layer (RNFL) and macular thicknesses can establish appropriate treatment timing in children with neurofibromatosis type 1 (NF1) with vision-threatening optic pathway gliomas (OPGs).⁽⁸⁴⁾

Toy laser macular burns in children

Raof et al reported that OCT imaging of persistent outer retinal layer disruption at the fovea in children exposed to laser toys.⁽⁸⁵⁾

Solar maculopathy

Symons et al reported that OCT imaging of loss of the hyper-reflective layer of the outer segment of the photoreceptors and loss of the inner portion of the hyper-reflective layer of the RPE in the fovea of a child after sun-gazing.⁽⁸⁶⁾

Spectral domain OCT is being used increasingly as a diagnostic and monitoring tool in children with visual loss. Because of short exposure durations and eye-tracking systems in devices such as the Heidelberg Spectralis. However, for the scans to be the most useful for detecting diseases in children, quantitative measures from children should be compared to age matched normal controls. Normal values from children are not currently available from manufacturers.⁽⁸⁷⁾